

Studies on Pion Dynamics at COMPASS: Pion Polarisability and Chiral Dynamics in $\pi\gamma \rightarrow 3\pi$

Jan Friedrich*[†] on behalf of the COMPASS collaboration

TU München

E-mail: jan.friedrich@ph.tum.de

The COMPASS experiment at CERN measures scattering reactions of muon and hadron beams of 160-200 GeV with high intensity and high resolution. Identifying very small momentum transfers to the target nuclei in pion-induced processes, the electromagnetic interaction is isolated and accesses pion-photon processes via the Primakoff effect.

In a dedicated beam time 2009, data have been taken for observing the pion-photon final state, i.e. effectively pion Compton scattering. The determination of the pion polarisability from these data is presented. The preliminary value is $\alpha_\pi = (1.9 \pm 0.7_{stat} \pm 0.8_{sys}) \cdot 10^{-4} \text{ fm}^3$, where the relation between electric and magnetic polarisability $\alpha_\pi = -\beta_\pi$ is assumed. This result is put in the context of the expectation from chiral perturbation theory and previous measurements. The potential of the data set taken in the year 2012, featuring higher statistics, is discussed.

Results and ongoing analyses of other final states involving chiral dynamics, such as 3-pion production in pion-photon collisions, which are also accessible at COMPASS, are presented as well.

Xth Quark Confinement and the Hadron Spectrum

8–12 October 2012

TUM Campus Garching, Munich, Germany

*Speaker.

[†]supported by the German ministry BMBF, the Maier-Leibnitz-Labor der LMU und TU München, and the DFG Cluster of Excellence “Origin and Structure of the Universe”

1. Pion-Photon reactions as test of Chiral Perturbation Theory

Properties of the pions (π^- , π^0 , π^+) are of crucial interest in understanding quantum chromodynamics (QCD), since the pion is the lightest system featuring confinement of quarks and gluons by the strong force. As such, the pions are identified in the framework of the low-momentum expansion of QCD, chiral perturbation theory (ChPT), as the Goldstone bosons emerging from the spontaneous breaking of chiral symmetry.

Pion-pion scattering has been studied in several approaches, *e.g.* in kaon decays, and successfully described within ChPT. In contrast, for pion-photon interactions even the most fundamental process of pion-photon (*i.e.* Compton) scattering has remained a riddle for the past 30 years: The leading structure-dependent term in this process is the polarisability, and its extraction from the first experimental data in 1983, confirmed by later experiments, resulted in values significantly higher than expected from most of the theoretical approaches. Clarifying this subject is the prime motivation for the experimental work presented here. On top of this, other pion-photon interactions with more pions in the final state came into reach, and are studied as well. This is, on the one hand, an independent research subject by itself, on the other hand, it represents a powerful check of the common aspects in the employed experimental techniques.

2. Embedding the process: Primakoff technique

Henry Primakoff proposed in 1951 [1] to make use of the intense electric field in the proximity of nuclei, which can be treated as a source of quasi-real photons, to study strongly-interacting particles. His original idea concerned the measurement of the π^0 lifetime by photon-photon fusion, but it was later realized that interactions of high-energetic hadrons with the nuclear Coulomb field represent similarly a scattering off the quasi-real photon density, and consequently the whole class of such hadron interactions is referred to as Primakoff reactions. The process is depicted in Fig. 1. The main contribution comes from impact parameters of the pions of a few nuclear radii, where the electric field is as strong as several 100 kV/fm. This displays how even a small polarisability as it is expected for hadrons can be measured as a modification of the cross-section for bremsstrahlung emission. The cross-section formula for a Primakoff reaction $\pi^- A \rightarrow X^- A$

$$\frac{d\sigma}{ds dQ^2 d\Phi} = \frac{\alpha}{\pi(s - m_\pi^2)} \cdot F_{\text{eff}}^2(Q^2) \cdot \frac{Q^2 - Q_{\text{min}}^2}{Q^4} \cdot \frac{d\sigma_{\pi\gamma}}{d\Phi} \quad (2.1)$$

bases on the factorization in the quasi-real photon density, which multiplies the cross-section $d\sigma_{\pi\gamma}/d\Phi$ for the real-photon subprocess $\pi^- \gamma \rightarrow X^-$. Mandelstam- s is the squared total energy in the $\pi^- \gamma$ subsystem, Q^2 is the momentum transfer to the nucleus, $\alpha = 1/137$ is the fine structure constant, m_π the rest mass of the charged pion, $Q_{\text{min}} = (s - m_\pi^2)/2p$ is the minimum momentum transfer for given s , and $F_{\text{eff}}^2(Q^2) \approx Z^2$ is the form factor of the target nucleus with charge Z . For the first process of interest, the final-state X^- is also $\pi^- \gamma$ and the subprocess is pion Compton scattering $\pi^- \gamma \rightarrow \pi^- \gamma$, for which the cross-section reads

$$\frac{d\sigma_{\pi\gamma}}{d\Omega_{cm}} = \frac{\alpha^2 (s^2 z_+^2 + m_\pi^4 z_-^2)}{s(s z_+ + m_\pi^2 z_-)^2} - \frac{\alpha m_\pi^3 (s - m_\pi^2)^2}{4s^2 (s z_+ + m_\pi^2 z_-)} \cdot \left(z_-^2 (\alpha_\pi - \beta_\pi) + \frac{s^2}{m_\pi^4} z_+^2 (\alpha_\pi + \beta_\pi) - \frac{(s - m_\pi^2)^2}{24s} z_-^3 (\alpha_2 - \beta_2) \right) \quad (2.2)$$

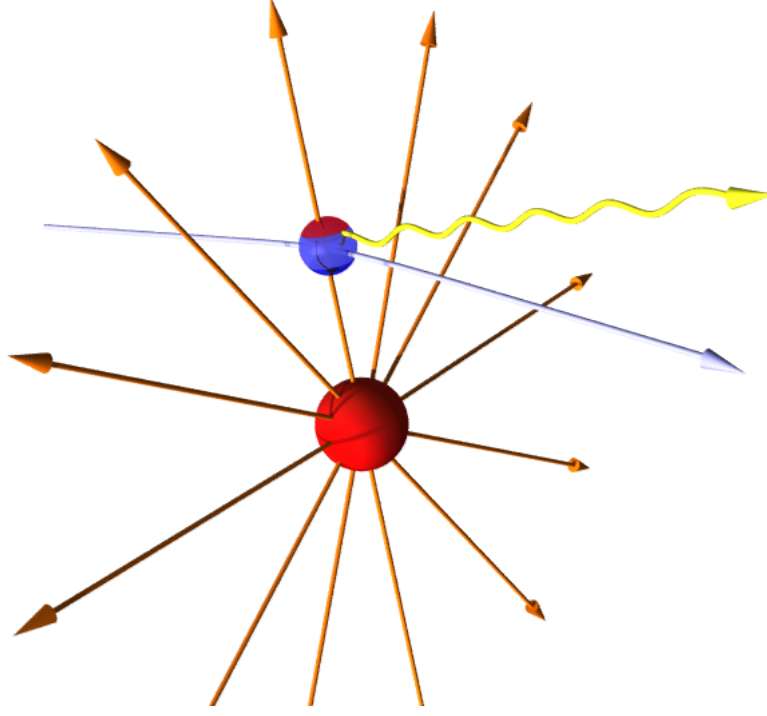


Figure 1: Visualization of the Primakoff Compton process: A high-energetic pion scatters in the electric field of a nucleus. For the magnetic contribution, it is to be realized that the nucleus passing the pion at high velocity represents an electric current inducing a magnetic field at the position of the pion.

where $z_{\pm} = 1 \pm \cos \theta_{cm}$ and θ_{cm} the scattering angle in the $\pi^- \gamma$ center-of-momentum system, and the pion structure enters through the electric and magnetic polarisabilities α_{π} and β_{π} , respectively. In the following, the sum $\alpha_{\pi} + \beta_{\pi}$ which is expected to be small, and also the influence of the quadrupole polarisabilities α_2 and β_2 is neglected. Then, the relative effect of the polarisability $\alpha_{\pi} = -\beta_{\pi}$ on the cross-section, Eq. 2.1, integrated in the small-momentum transfer region $Q^2 \leq 10^{-3} \text{ GeV}^2/c^2$ and depending only on the fraction of energy transferred from the incoming pion beam to the emitted photon, $x_{\gamma} = E_{\gamma}/E_{beam}$, can be simplified into

$$R = \frac{\sigma(x_{\gamma})}{\sigma_{\alpha_{\pi}=0}(x_{\gamma})} = 1 - \frac{3}{2} \cdot \frac{m_{\pi}^3}{\alpha} \cdot \frac{x_{\gamma}^2}{1-x_{\gamma}} \alpha_{\pi} \quad (2.3)$$

This relation is used to extract the polarisability from the measurement of the photon energy spectrum in the the Primakoff process $\pi^- Z \rightarrow \pi^- \gamma Z$ on a nucleus with charge Z , as it has been done in the first measurement of this kind at Serpukhov [2].

3. Pion polarisability measurement at COMPASS

The COMPASS experiment deploys secondary hadron and tertiary muon beams from the CERN 450 GeV super proton synchrotron (SPS). Its multi-purpose detector concept allows for

a wide range of investigations in hadron physics, with high-precision and high-rate capable tracking, particle identification and calorimetry in its two-stage magnetic spectrometer setup. For a more detailed description and results on hadron spectroscopy the reader is referred to [3].

The measurement of the pion polarisability has been one of the original goals of the proposal for the COMPASS experiment. After a pilot run in the year 2004, the data presented in the following have been collected in a two-week beam time in 2009, with significant improvements in the calorimetry and the trigger system which based on the detailed analysis of the 2004 data. One of the conclusions along with preparing the data taking in 2009 [4] was that lead is not a favorable target material despite the high nuclear charge Z , since the radiative corrections due to multiple photon exchange and screening are large and represent a non-negligible source of systematic uncertainty. Consequently, the measurement was performed with a 3 mm thick nickel disk as nuclear target.

The employed 190 GeV negative-charge hadron beam contains to more than 98% pions, which are distinguished from kaons by Cherenkov detectors [3]. A unique feature of the pion polarisability measurement at COMPASS is that the beam can be switched, within about an hour, from hadron to muon beam, and the spectrometer is specialized to muon identification due to the broad physics program with muon beams. For the polarisability measurement, this allows for control measurements with muon beam, for which the theoretical expectation of the relevant bremsstrahlung process $\mu^- \text{Ni} \rightarrow \mu^- \gamma \text{Ni}$ is completely determined by quantum electrodynamics (QED).

Reactions of the type $\pi^- \text{Ni} \rightarrow \pi^- \gamma \text{Ni}$ are selected by requiring the measurement of one negatively-charged scattered particle trajectory, that forms with the incoming pion trajectory a vertex consistent with an interaction in the nickel target, and a high-energetic shower in the electromagnetic calorimeter (ECAL), by which energy and momentum direction of the emitted photon can be reconstructed. Exclusive reactions are selected by energy conservation in the process $\pi^- \text{Ni} \rightarrow \pi^- \gamma \text{Ni}$ as depicted in Fig. 2, the upper-left graph showing the peak attributed to exclusive events in $\Delta E = E_{beam} - E_{\pi'} - E_{\gamma} \approx 0$, neglecting the (tiny) nuclear recoil energy. The width of the peak $\sigma \approx 2.6$ GeV is well in agreement with the simulation, reflecting mainly the resolution of the ECAL. The pion data show a non-exclusive background contribution, visible as a tail at negative values of ΔE . Those stem from diffractive processes, mainly those with neutral pions in the final state, leading to a very similar ECAL response as the intended single-photon events. Their contribution is not included in the simulation, instead it is estimated from events with identified π^0 . The result is a fraction of about 5%, slightly depending on the photon energy (top-right graph in Fig. 2), and is subtracted in the further analysis steps. The muon data do not feature such diffractive contributions. Their exclusivity peak is in full agreement with the simulation, and has a similar width as that of the pion data.

Photon exchange is identified by the strong increase of interaction probability at extremely small momentum transfer, as given by the quasi-real photon density term of Eq. 2.1. This ‘‘Primakoff peak’’ enters in the usual q^2 distribution, shown in the bottom-left graph of Fig. 2, only in the very first bin. Its details are better displayed in the variable $|Q| = |\vec{q}|$ shown in the bottom-right graph. The peak position as given by Eq. 2.1 would be around 1 MeV/c, however in the data it is smeared with the experimental resolution of about 10 MeV/c. On the scale of the incoming beam momentum of 190 GeV/c, this is an excellent value stemming from an angular resolution for the photon and the scattered pion with respect to the incoming pion direction of about 30 μrad . This is reached by determining the position of the electromagnetic showers of the photons in the ECAL,

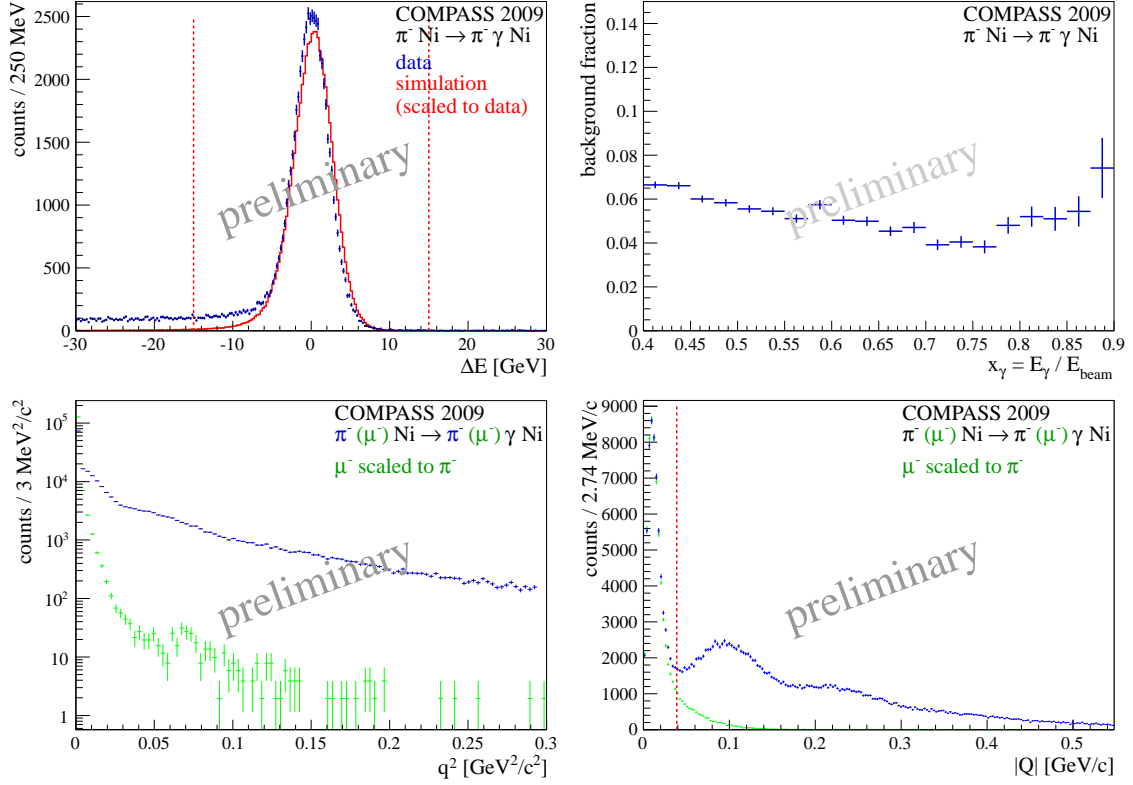


Figure 2: Energy balance of the reaction $\pi^- \text{Ni} \rightarrow \pi^- \gamma \text{Ni}$ (top left), background fraction (top right), and momentum transfer spectra in q^2 and $|Q|$ (bottom left and right, respectively) compared to those of the $\mu^- \text{Ni} \rightarrow \mu^- \gamma \text{Ni}$ control measurements. The cuts applied to the data are indicated as vertical dashed lines.

about 32 m downstream of the target, with a spatial resolution of 1.2 mm, and the track of the scattered pion with a spatial resolution of about $10 \mu\text{m}$ in the microstrip silicon detectors employed about 0.5 m downstream of the target. These features of the $|Q|$ distribution are also well described by the simulation, which fully matches in the muon case and lacks the salient additional pattern due to diffractive processes in the pion case. Photon exchange is selected by the cut indicated in the $|Q|$ distribution.

For the determination of the polarisability, the photon energy spectrum is examined according to Eq. 2.3. In the case of muon beam, the shape of the distribution is in excellent agreement with the simulation as shown in the upper graphs of Fig. 3. The size of the “false polarisability” signal, in agreement with zero within the fit uncertainty, of $\pm 0.6 \cdot 10^{-4} \text{ fm}^3$ is taken as an estimate for apparatus imperfections not described by the simulation, *e.g.* concerning the tracking.

In the case of pion beam, the experimental spectrum has been corrected for the background estimation shown in Fig. 2, and is divided by the simulation, in which the bremsstrahlung cross-section for a pointlike spin-0 boson has been taken. The result of this procedure is shown in the lower graphs of Fig. 3. By fitting the distribution according to Eq. 2.3, the pion polarisability is determined from the COMPASS 2009 data to be $\alpha_\pi = (1.9 \pm 0.7_{\text{stat}}) \cdot 10^{-4} \text{ fm}^3$.

Radiative corrections have been applied on the level of the simulation event-by-event accord-

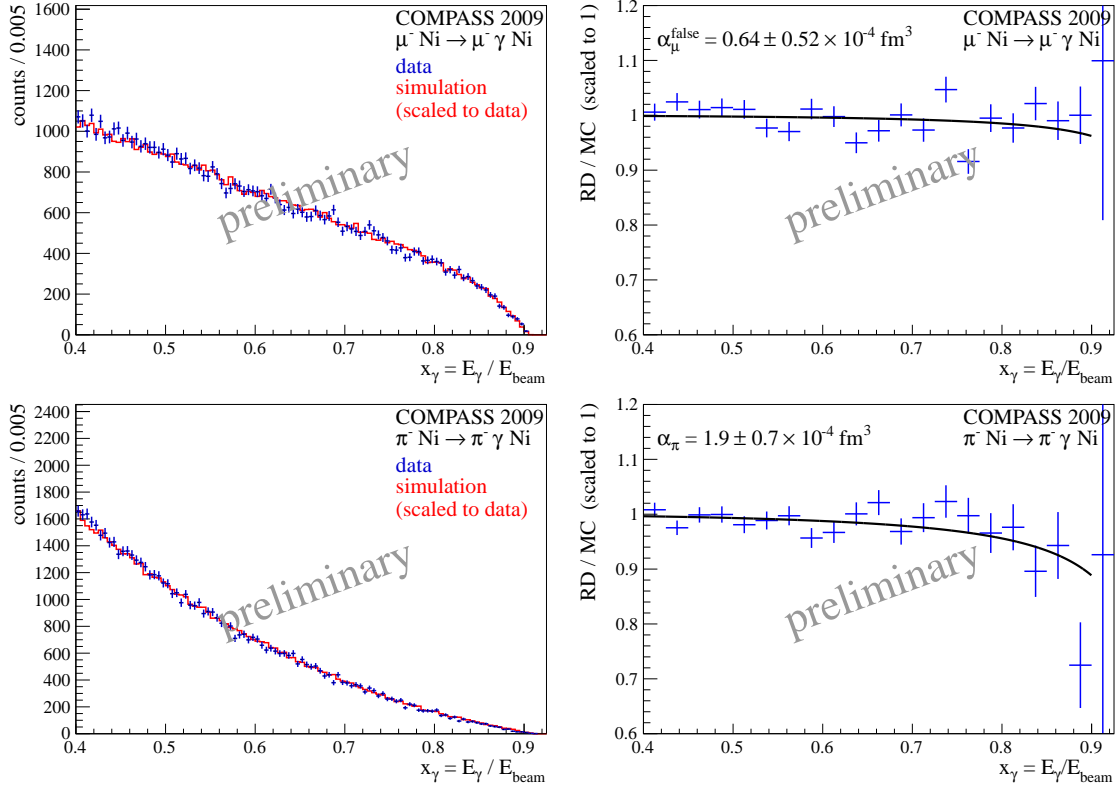


Figure 3: Control measurement with muons $\mu^- \text{Ni} \rightarrow \mu^- \gamma \text{Ni}$ (top) and determination of the pion polarisability through the process $\pi^- \text{Ni} \rightarrow \pi^- \gamma \text{Ni}$ (bottom).

ing to [5] for the pion case, and to [6] for the muon case. Their effect on the level of the polarisability signal has been determined to be about $\pm 0.3 \cdot 10^{-4} \text{ fm}^3$ and this value has been included in the list of systematic uncertainties in Tab. 1, since a cross-check of the corrections is still ongoing.

An additional background contained in the data stems from scattering of the beam particles off the electrons in the target. Since the recoiling electrons may lose practically all their energy by bremsstrahlung, this leads to a signature very similar to the intended process of photon emission when scattering off the nuclei. The contribution of this process has been investigated, and its impact on the polarisability determination included as systematic uncertainty in Tab. 1.

Summing all discussed systematic uncertainty contributions as summarized in Tab. 1, leads to a total of $\pm 0.8 \cdot 10^{-4} \text{ fm}^3$. So, the preliminary COMPASS result for the pion polarisability from the 2009 data is

$$\alpha_\pi = (1.9 \pm 0.7_{\text{stat}} \pm 0.8_{\text{sys}}) \cdot 10^{-4} \text{ fm}^3 \quad (3.1)$$

4. Discussion of the polarisability result

The presented preliminary COMPASS value for the pion polarisability is compared to previous experimental results in Fig. 4. Historically (left graph) the first result obtained at Serpukhov [2] had been confirmed much later by the dedicated experiment on radiative pion photoproduction

source of systematic uncertainty	estimated magnitude
tracking	0.6
radiative corrections	0.3
background subtraction in Q	0.4
pion-electron scattering	0.2
quadratic sum	0.8

Table 1: Systematic uncertainty estimates for the pion polarisability measurement (on 68% confidence level).

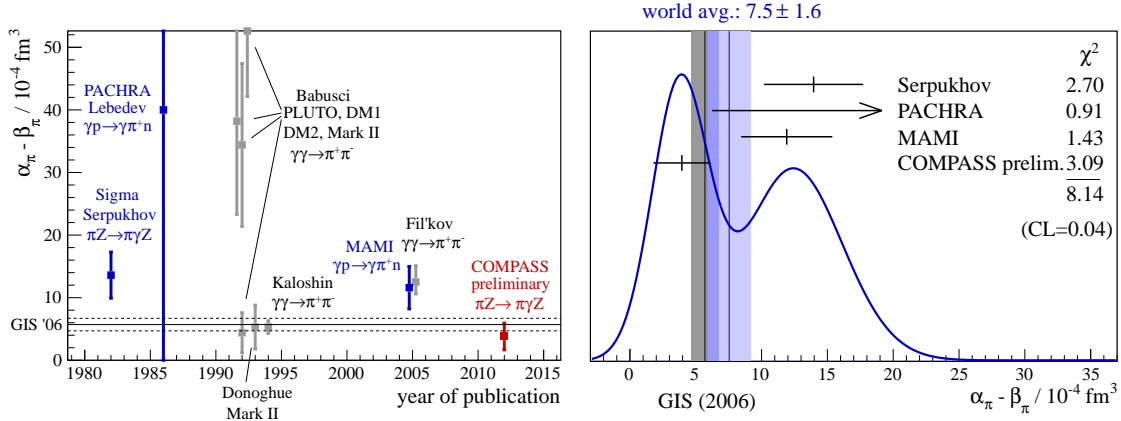


Figure 4: Placement of the preliminary COMPASS result on the pion polarisability in the world data (left) and the ideogram in “PDG style” [13] (right). Plots from [14].

at MAMI [7]. In the mean time, the available data on $\gamma \gamma \rightarrow \pi^+ \pi^-$ at $e^- e^+$ -colliders were re-interpreted by several authors [8, 9, 10, 11] claiming very different values for the pion polarisability, inspired by the assumptions on pion dynamics and the related low-energy constants that enter in this interpretation.

In that regard, the COMPASS result is in significant tension with the earlier experimental determinations of the pion polarisability, as the ideogram representation in Fig. 4 (right) shows, where only the dedicated experiments for the pion polarisability are included. Instead, the new result is found in good agreement with the expectation of chiral perturbation theory [12].

In view of the small value obtained for the pion polarisability in this analysis, it is of highest interest what the data taken in the year 2012 at COMPASS with a very similar setup as described here will show. For this data set, the statistical uncertainty is expected to be a factor of three smaller and the polarisability signature of Fig. 3 accordingly clearer. This data set will also allow the extraction of α_π and β_π independently, as well as the determination of the quadrupole polarisability $\alpha_2 - \beta_2$. In addition, the first value for the kaon polarisability is in reach, using the identified kaon component of the beam and employing the same analysis technique as for the pion.

5. Further chiral dynamics processes

Along with refining the analysis methods described above, further processes on chiral dynamics that may be in reach with the COMPASS data were investigated [15]. Since long, the chiral anomaly in the process $\pi^- \gamma \rightarrow \pi^- \pi^0$ is of interest, however the analysis of this channel is still underway.

The detailed study of two-pion production at low energy, is also not yet finished for the neutral-pion case $\pi^- \gamma \rightarrow \pi^- \pi^0 \pi^0$. For the charged case $\pi^- \gamma \rightarrow \pi^- \pi^+ \pi^-$, however, the analysis [16] of the data from the pilot run in 2004 has been completed and published [17]. Here, the absolute cross-section for the process has been determined in five bins of the final-state mass from threshold at $3m_\pi$ up to $5m_\pi$, employing the partial-wave analysis techniques from the hadron spectroscopy program [3]. The experimental data confirm the expectation from tree-level ChPT on the level of the experimental uncertainty of 20%. This confirms, on the one hand, the extension of the ChPT approach for processes involving the coupling of four pions, *i.e.* the leading order, to processes involving an additional coupling to a photon. On the other hand, it demonstrated that the Primakoff technique in the form of Eq. 2.1 can be safely employed. In terms of studying ChPT, the neutral channel $\pi^- \gamma \rightarrow \pi^- \pi^0 \pi^0$ will be of higher relevance, since for this channel higher-order loop corrections are expected to play a larger role [18].

References

- [1] H. Primakoff, Phys. Rev. **81**, 899 (1951).
- [2] Yu. M. Antipov *et al.*, Phys. Lett. **B121**, 445 (1983).
- [3] B. Grube, “Hadron Spectroscopy in COMPASS”, these proceedings
- [4] N. Kaiser and J. M. Friedrich, Eur. Phys. J. **A39**, 71 (2009).
- [5] N. Kaiser and J. M. Friedrich, Nucl. Phys. **A812**, 186 (2008).
- [6] N. Kaiser, Nucl. Phys. **A837**, 87 (2010).
- [7] J. Ahrens *et al.*, Eur. Phys. J. **A23**, 113 (2005).
- [8] D. Babusci *et al.*, Phys. Lett. **B277**, 158 (1992).
- [9] J. F. Donoghue and B. R. Holstein Phys. Rev. **D48**, 137 (1993).
- [10] A. E. Kaloshin and V. V. Serebryakov, Z. Phys. **C64**, 689 (1994).
- [11] L. V. Fil’kov and V. L. Kashevarov, Phys. Rev. **C73**, 035210 (2006).
- [12] J. Gasser, M. A. Ivanov and M. E. Sainio, Nucl. Phys. **B745**, 84 (2006).
- [13] J. Beringer *et al.* [Particle Data Group], Phys. Rev. **D86**, 010001 (2012).
- [14] T. Nagel, PhD thesis, Tech. Univ. München (2012), CERN-THESIS-2012-138, <http://cds.cern.ch/record/1484476>.
- [15] N. Kaiser and J. M. Friedrich, Eur. Phys. J. **A36**, 181 (2008).
- [16] S. Grabmüller, PhD thesis, Tech. Univ. München (2012), CERN-THESIS-2012-170, <http://cds.cern.ch/record/1492155>
- [17] C. Adolph *et al.* [COMPASS Collaboration] Phys. Rev. Lett. **108**, 192001 (2012).
- [18] N. Kaiser, Nucl. Phys. **A848**, 198 (2010).